

## Solvation Effects and Inhomogeneous Broadening in Optical Spectra of Phenol Blue

Francesca Terenziani and Anna Painelli\*

Dipartimento di Chimica GIAF, Università di Parma, I-43100 Parma, Italy

Davide Comoretto

INFN, Dipartimento di Chimica e Chimica Industriale, Università di Genova, I-16146 Genova, Italy

Received: April 26, 2000; In Final Form: September 14, 2000

Electronic and vibrational spectra of phenol blue dissolved in a few solvents are carefully analyzed on the basis of a simple theoretical model accounting for electron–molecular vibration coupling and for solvation. Nonresonant Raman and electronic absorption spectra measured in a series of solvents with similar refractive index and increasing dielectric constant are the basis to extract a reliable set of microscopic parameters. On the basis of these parameters, we reproduce the large and impressive inhomogeneous broadening effects observed in resonant Raman spectra collected in polar solvents. Solvation effects on the first hyperpolarizability are also discussed.

## Introduction

Phenol blue (PB, also known as dimethylindooaniline, see Figure 1) is a commercial dye whose interesting solvatochromic properties are known since the early 40's.<sup>1</sup> In the 70's an extensive study of its electronic absorption spectrum in different solvents and solvent mixtures has been reported,<sup>2</sup> aimed to disentangle solvent polarity effects from those possibly arising from solute–solvent H-bond interactions. In recent years, these studies have been extended to include supercritical fluids as solvents,<sup>3</sup> offering the opportunity to investigate solvent density effects. Moreover, detailed quantum chemistry calculations have been reported, investigating the role of the solvent on PB properties.<sup>4</sup> PB is an interesting chromophore for NLO applications too, as proved by its large first hyperpolarizability.<sup>5</sup> In fact the two limiting resonating structures (see Figure 1) describing the molecule have similar energy (the two rings simply reverse their benzenoid–quinonoid nature) and both contribute appreciably to the ground state (gs).

As widely discussed in the companion paper<sup>6</sup> (hereafter referred as I), the large  $\beta$ -response of PB implies large nonperturbative solvation effects in both electronic and vibrational spectra. Large nonperturbative solvation effects are typically recognized from nonspecular absorption and emission spectra, with narrower emission than absorption bands.<sup>7</sup> PB is a nonfluorescent dye, so that its nonlinearity is hardly recognized in electronic spectra. In fact both the solvatochromism and the inhomogeneous broadening of absorption bands of push–pull chromophores can be easily reproduced in effective models accounting for linearized solute–solvent interaction.<sup>6</sup> On the other hand, nonlinearity stems out apparently from vibrational spectra. Yamaguchi et al. recently reported<sup>8</sup> resonant Raman (RR) spectra of PB: in polar solvents a couple of vibrational modes show large dispersion with the excitation line, whereas in apolar solvents RR lines show the standard nondispersive behavior. By combining extensive experimental investigation<sup>8</sup> with theoretical study,<sup>9</sup> Yamaguchi et al. were able to show

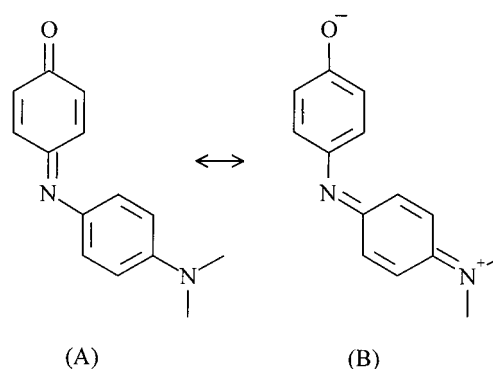
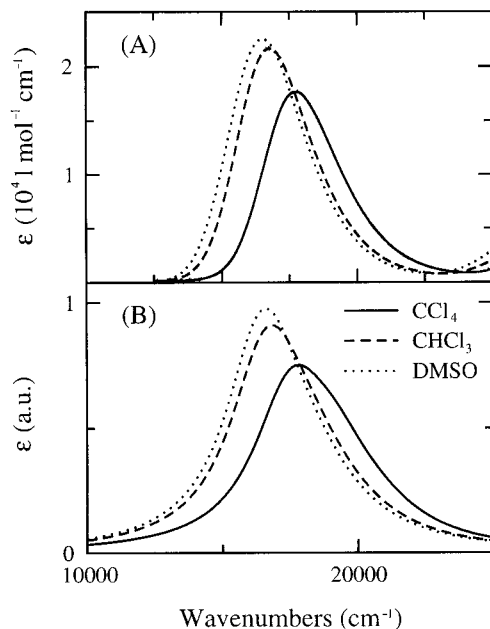


Figure 1. Resonating structures of phenol blue.

that the observed dispersion of RR frequencies in polar solvents originates from inhomogeneous broadening of both electronic and vibrational energies, as due to disorder in the solvation cage. Indeed, they recognized that the dispersion of RR lines can only be understood if the fluctuations of electronic and vibrational energies due to disorder are correlated. However, Yamaguchi et al. adopted a standard rigid-solute picture for the solute–solvent interaction, and were therefore forced to introduce empirically the correlation between electronic and vibrational energies, by imposing an ad hoc dependence of the vibrational frequency on the solvation coordinate. Whereas the model satisfactorily reproduces most of experimental features, it cannot shed light on the physics underlying the correlation of electronic and vibrational energies, that instead stems out quite naturally in the model for push–pull chromophores discussed in I, properly accounting for the intrinsic nonlinearity of these molecules.

In this paper we adopt the model presented in I to describe solvent effects in electronic and vibrational spectra of PB. To compare with as many experimental data as possible, we recorded nonresonant Raman (NRR) spectra of PB in a few solvents, as reported in section 3. In fact, as it is the case for many systems with large electron–phonon coupling,<sup>10–12</sup> vibrational spectroscopy is a very useful tool to investigate the behavior of push–pull chromophores too. In section 4 we briefly

\* Corresponding author: Phone: +39-0521-905461. Fax: +39-0521-905556. E-mail: painelli@unipr.it.



**Figure 2.** Experimental (A) and calculated (B) electronic spectra of PB in  $\text{CCl}_4$  (full line),  $\text{CHCl}_3$  (dashed line), and DMSO (dotted line). On the y-axis the molar absorption coefficient ( $\epsilon$ ) is reported. The simulated spectra have been calculated for the parameters reported in Table 2, with an intrinsic electronic line width of  $1600\text{ cm}^{-1}$  (HWHM).

review the model and, by comparing experimental and simulated spectra, we fix the microscopic parameters relevant to PB. An extensive discussion of the results is reported in section 5. Fixed a few model parameters, solvent effects on electronic absorption spectra, on NRR spectra as well as on RR spectra, including their anomalous dispersion with the excitation line, are all reproduced in a unitary frame. Since our model makes no special assumptions on PB, it applies more generally to push-pull chromophores, and we hope this work will trigger some interest in vibrational studies of this class of molecules.

### Experimental Section

Phenol blue was purchased from Aldrich and used without further purification. Solutions were prepared in spectrophotometric grade  $\text{CCl}_4$ ,  $\text{CHCl}_3$ , and dimethyl sulfoxide (DMSO). Electronic absorption spectra of  $\sim 10^{-4}$  M PB solutions were measured with both a Uvidec-505 and a Perkin-Elmer Lambda 9 spectrophotometers.

Non resonant Raman (NRR) spectra have been recorded with a Bruker FRS 100 FT spectrometer with Nd:YAG excitation at 1064 nm. The spectra were averaged over 2000 scans and collected at room temperature with resolution of  $2\text{ cm}^{-1}$ . We present NRR spectra obtained for solutions  $10^{-2}$  M: at this concentration the signal-to-noise ratio is good, whereas spectra are not affected by aggregation effects, as demonstrated by the comparison with spectra collected on solution  $10^{-3}$  M. Raman spectra have not been corrected for the instrumental response. Preliminary RR spectra have also been recorded on solution  $\sim 10^{-3}$  M with Raman spectrometer Dilor Mod. Labram, equipped with a He-Ne laser.

### Results

Figure 2A shows the absorption spectra of PB dissolved in  $\text{CCl}_4$ ,  $\text{CHCl}_3$  and DMSO. In  $\text{CCl}_4$  the absorption band is peaked at  $17750\text{ cm}^{-1}$ , while in polar solvents it shifts at  $16800$  and  $16500\text{ cm}^{-1}$  for  $\text{CHCl}_3$  and DMSO, respectively. This red-shift of the absorption maximum with increasing solvent polarity is

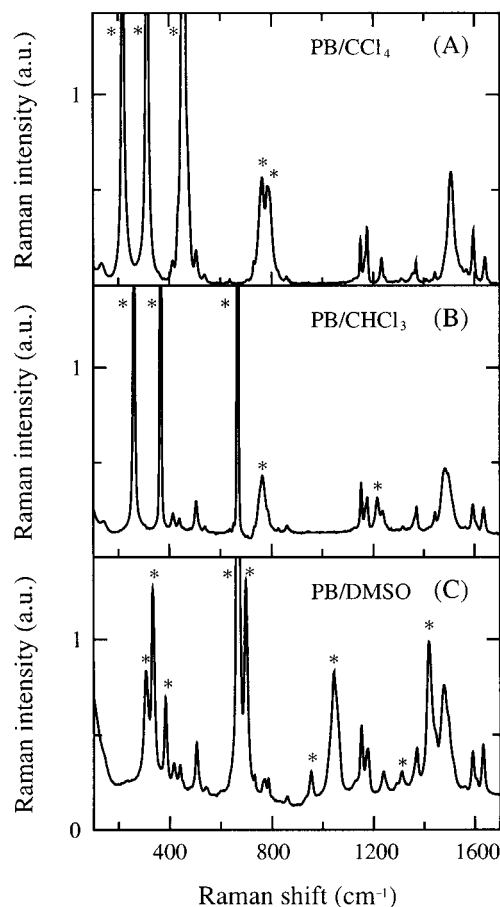


**Figure 3.** Nonresonant Raman spectra of PB in  $\text{CCl}_4$  (A),  $\text{CHCl}_3$  (B), and DMSO (C). Stars mark solvent bands; the units on y-axis are the same in the three panels.

accompanied by a corresponding increase of the oscillator strength from 0.8 in  $\text{CCl}_4$  to 1.0 in  $\text{CHCl}_3$  to 1.1 in DMSO.

Figure 3 shows the NRR spectra of PB solutions in  $\text{CCl}_4$  (A),  $\text{CHCl}_3$  (B), and DMSO (C) in the  $100\text{--}1700\text{ cm}^{-1}$  spectral range. In the figure the Raman intensities on the y-axis are shown in the same arbitrary units in the three panels, so that the relative intensities of NRR bands in the three solvents can be reliably compared. Several bands are detected, in addition to those of solvents, whose Raman shifts are summarized in Table 1. The assignment of these bands, tentatively reported in ref 3 by means of RR spectroscopy, is beyond the aim of this work. Here we focus attention on the spectral region  $1300\text{--}1700\text{ cm}^{-1}$  (Figure 4A) where two bands at  $\sim 1500$  and  $\sim 1640\text{ cm}^{-1}$  assigned to  $\text{C}=\text{N}$  and  $\text{C}=\text{O}$  stretching modes, respectively,<sup>3</sup> show a strong dependence on the solvent polarity. The lower band shifts by  $29\text{ cm}^{-1}$  (from  $1507\text{ cm}^{-1}$  in  $\text{CCl}_4$  to  $1483\text{ cm}^{-1}$  in  $\text{CHCl}_3$  to  $1478\text{ cm}^{-1}$  in DMSO); the higher one moves by  $10\text{ cm}^{-1}$  (from  $1642\text{ cm}^{-1}$  in  $\text{CCl}_4$  to  $1636\text{ cm}^{-1}$  in  $\text{CHCl}_3$  to  $1632\text{ cm}^{-1}$  in DMSO). Notice also that the  $\sim 1500\text{ cm}^{-1}$  band considerably broadens with increasing solvent polarity. Our preliminary RR spectra agree with the partial data reported in refs 3 and 8. The comparison of NRR and RR spectra (not shown here) in the three solvents in the whole investigated spectral range ( $100\text{--}3500\text{ cm}^{-1}$ ) confirms that by far the largest solvation effects are observed for the two modes at  $\sim 1500$  and  $\sim 1640\text{ cm}^{-1}$ .

### Theoretical Model

We study optical spectra of PB dissolved in  $\text{CCl}_4$ ,  $\text{CHCl}_3$ , and DMSO, three solvents with similar refractive indices (1.460,

**TABLE 1: Raman Shift Recorded for PB Dissolved in CCl<sub>4</sub>, CHCl<sub>3</sub>, and DMSO<sup>a</sup>**

PB/CCl <sub>4</sub>	PB/CHCl <sub>3</sub>	PB/DMSO
133 vw 217.9 s (*)	140.25 vw 261.3 s (*)	142.5 sh
314.3 s (*)		306.6 m (*)
365 sh	366.4 vs (*)	333.6 m (*)
413.1 w	413.6 w 438.7 w	382.8 m (*) 415.5 vw 439.6 vw
445 sh (*) 459.9 vs (*) 504.7 w 538.0 w 636.3 vw	504.7 w 539.4 vw 635.9 vw 651.8 w (*) 667.2 vs (*)	504.7 w 540.4 vw
		668.6 s (*) 698.5 m (*)
705.3 vw 731.8 w 764.4 m (*)	704.8 vw 731.8 vw 764.1 m (*)	731.3 vw
784.4 m (*)		770.9 vw
824.9 vw 859.1 vw	784.8 sh 826.3 vw 860.5 vw	785.8 vw
		859.6 vw 953.6 m (*) 1043.3 m (*) 1127 sh 1151.7 w
1120 sh 1150.3 w 1165 sh 1176.3 w	1152.7 m 1168 sh 1176.3 m 1216.3 m (*)	1176.3 w
1233.2 w 1246 sh 1311.3 vw	1236.6 m	1239 vw
	1317.1 vw 1362 sh 1371.1 m	1311.3 vw (*)
1358.1 w 1369.2 w 1411.1 vw		1370.6 w
	1444.4 w 1483.4 m 1495 m (*?)	1418.8 m (*) 1443 sh 1478.1 m
1507 m		1515 sh
1550 sh (*) 1568.3 w 1595.8 w	1563.5 vw 1593.8 w	1591.4 w
1642 w	1605 sh 1635.8 w	1607 sh 1632.4 w

<sup>a</sup> (\*) marks solvent bands; (\*?) marks overlapping solute and solvent bands.

1.446, and 1.430, respectively at 20 °C) and increasing polarity (the dielectric constants are 2.238, 4.806, and 46.7, respectively at 20 °C). According to the model discussed in I, we therefore assume fixed molecular parameters and account for the increasing solvent polarity by increasing the solvent orientational relaxation energy,  $\epsilon_{or}$ . This parameter, measuring the energy gain due to the relaxation of slow (orientational) degrees of freedom of the solvent when the solute structure varies from neutral to zwitterionic, can be estimated from the properties of the solvent (dielectric constant and refractive index) provided a microscopic model for the solute–solvent interaction is defined.<sup>13</sup> We prefer however to treat  $\epsilon_{or}$  as an empirical parameter to be extracted from experimental data. In the self-consistent DA dimer model, the electronic spectra of a solvated push–pull chromophore are fully described in terms of three

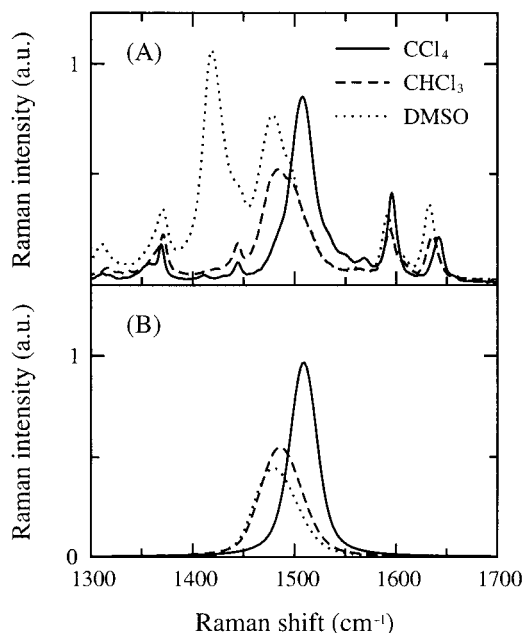


**Figure 4.** Detail of the experimental (A) and calculated (B) nonresonant Raman spectra of PB in CCl<sub>4</sub>, CHCl<sub>3</sub>, and DMSO. The simulated spectra have been calculated with the parameters in Table 2, and an intrinsic vibrational line width of 8 cm<sup>-1</sup> (HWHM). All calculated spectra are reported on the same arbitrary scale of intensity.

parameters:  $z_0$ ,  $\sqrt{2}t$ , and  $\epsilon_T$ . The first two parameters describe the two-state problem,  $2z_0$  being the vertical energy gap between  $|D^+A^- \rangle$  and  $|DA \rangle$ , and  $\sqrt{2}t$  the matrix element connecting the two states. The total relaxation energy,  $\epsilon_T$ , is the sum of the energy gained by  $|D^+A^- \rangle$  due to the relaxation of orientational degrees of freedom of polar solvents ( $\epsilon_{or}$ ), plus that due to the relaxation of coupled internal vibrations ( $\epsilon_{sp}$ ). The three parameters relevant to electronic spectra,  $z_0$ ,  $\sqrt{2}t$ ,  $\epsilon_T$ , can be fixed if a complete set of experimental data is available for a few solvents: specifically absorption and emission frequencies, oscillator strengths and gs dipole moments are required. Not all these data are available for PB: the gs dipole moment has only been estimated in benzene,<sup>1</sup> and since PB is not fluorescent, emission frequencies are not known. From the available experimental data we cannot get a unique set of microscopic parameters but, by comparing electronic and vibrational spectra, we can make an educated guess of the model parameters. In the following we do not claim having extracted the best parameter set for PB: in fact our aim is to demonstrate that the interesting and complex spectral behavior of PB can be described within the model presented in I, adopting a plausible set of microscopic parameters.

Available theoretical and/or experimental estimates of  $\sqrt{2}t$  for push–pull chromophores locate it around 1 eV.<sup>7,14–16</sup> for the sake of simplicity we then fix  $\sqrt{2}t = 1$  eV. In the following, all energies are given as dimensionless quantities, to mean they are measured in  $\sqrt{2}t$  units, or, equivalently, in electronvolts. Within the dimer model, once the energy units are fixed, the electronic absorption frequency ( $\omega_{CT}$ ) unambiguously determines the product  $\rho(1 - \rho)$ , with  $\rho$  measuring the chromophore polarity, i.e., the weight of  $|D^+A^- \rangle$  in the gs.<sup>7</sup> Since PB is a positive solvatochromic dye (i.e.,  $\omega_{CT}$  red-shifts with increasing solvent polarity, see Figure 2A) and has a positive  $\beta$ ,<sup>5</sup> then  $\rho < 0.5$ .<sup>7</sup> The experimental  $\omega_{CT}$  deduced from the spectra in CCl<sub>4</sub>, CHCl<sub>3</sub>, DMSO reported in Figure 2A fix the corresponding  $\rho$  as 0.26, 0.33 and 0.35, respectively. These values, related to the choice of  $\sqrt{2}t$ , are by no means unique,

**TABLE 2: Molecular Parameters and the Three  $\epsilon_{or}$  Corresponding to the Three Solvents of Interest**

$z_0$	$\omega_1$	$\epsilon_1$	$\epsilon_{or}$		
			CCl <sub>4</sub>	CHCl <sub>3</sub>	DMSO
0.7	0.20	0.42	0.2	0.6	0.7

nevertheless they are plausible: they locate in fact PB in the  $\rho$  region maximizing the  $\beta$  response, as supported by the large  $\beta$  values measured for PB with respect to similar dyes.<sup>5</sup> Larger  $\rho$  are not plausible either in DMSO: in fact at  $\rho \sim 0.5$  our model predicts the vanishing of the NRR intensity of coupled modes, whereas experimental data (Figures 3 and 4A) do not show any important effect in relative NRR intensities. Recent quantum chemistry calculations combined with spectroscopic analysis<sup>4</sup> demonstrate that, even in highly polar solvents, the quinoneimine form ((A) in Figure 1) gives the largest contribution to the gs of PB, then further supporting our assignment of  $\rho < 0.5$  even in DMSO.

Because of the lack of experimental data on emission frequencies, we cannot extract from electronic spectra both  $z_0$  and  $\epsilon_T$ , even if in each solvent the relation between the two is fixed by the corresponding  $\rho$ . More information can be gained from vibrational spectra. Both in the RR spectra reported by Yamaguchi et al.<sup>3,8</sup> and in the NRR spectra in Figure 4A, the largest solvation effects are observed for the vibration at  $\sim 1500$   $\text{cm}^{-1}$ . As a first approximation we then discuss PB in the hypothesis of a single coupled vibration. The extension to two coupled modes, as required to describe the small solvation effects observed for the C=O stretching mode around 1640  $\text{cm}^{-1}$ , is shortly discussed in the next section. Modeling vibrational spectra requires detailed information about the relevant vibration, in particular the reference vibrational frequency  $\omega_1$ , and the corresponding relaxation energy  $\epsilon_1 = \epsilon_{sp}$ , are needed. Overall we need three molecular parameters,  $z_0$ ,  $\omega_1$ , and  $\epsilon_{sp}$ , independent of the solvent polarity, plus the three  $\epsilon_{or}$  values relevant to the three solvents of interest (the parameter  $\epsilon_T$  is easily obtained as  $\epsilon_{sp} + \epsilon_{or}$ ). The values of the six parameters, summarized in Table 2, are chosen to reproduce the three NRR frequencies and the three electronic absorption frequencies.

The fit is far from unique, but the chosen parameter set works well, reproducing not only the experimental frequencies, but also the intensities and the band-shapes, as shown in Figures 2 and 4. The electronic spectra in Figure 2B are calculated by imposing a Lorentzian line shape for the intrinsic absorption line, with half width at half-maximum (HWHM) of 1600  $\text{cm}^{-1}$ . The evolution of the absorption band-shape with the solvent polarity is well reproduced, and the fairly broad wings in calculated spectra originate from our choice of a Lorentzian shape for vibronic bands. A better fit can be obtained in terms of Gaussian shapes.<sup>17</sup> The fairly large intrinsic line width compares favorably with that estimated from absorption spectra of polar chromophores with resolved vibronic structure (see, e.g., ref 18), and can be related to the fast oscillations of the reaction field as due to the electronic component of the solvent polarization. To model NRR spectra, we choose a Lorentzian shape as the intrinsic vibrational line shape, with HWHM  $\gamma = 8$   $\text{cm}^{-1}$ . The choice of the intrinsic line width for the electronic transition is not critical, but our choice for the vibrational line width deserves some comment. We fixed the vibrational line width on the basis of the observed line width of NRR bands relevant to noncoupled modes. With this choice, however, we cannot reproduce the fairly large width of the NRR band observed in CCl<sub>4</sub>, unless we assign, even to this nonpolar

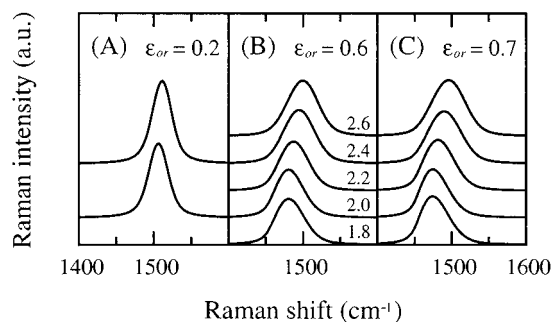


**Figure 5.** Resonant Raman spectra calculated with the same parameters as in Figures 2 and 3, for three solvent polarities ( $\epsilon_{or}$ ). The spectra are labeled by the frequency of the excitation photon (expressed in electronvolts).

solvent, a small  $\epsilon_{or}$ , as reported in Table 2. This small value of the effective orientational relaxation energy in a nonpolar solvent can be justified in microscopic models for solute–solvent interaction accounting for quadrupolar, or higher order contributions to the reaction field.<sup>18</sup> In a more suggestive hypothesis,  $\epsilon_{or}$  can account for the presence, at very low frequencies (typically the far-infrared region), of internal molecular vibrations coupled to the electrons. These vibrations, which in the case of PB possibly involve a rotation around the central C–N bond, are felt, by the vibrations in the 1400–1600  $\text{cm}^{-1}$  spectral region, as slow motions that essentially have the same (broadening) effects as the orientational degrees of freedom of a polar solvent. Both mechanisms can of course contribute to the broadening of vibrational lines observed in CCl<sub>4</sub>. The assessment of their relative importance requires a systematic study of vibrational line shapes in several nonpolar solvents.

The same parameters adopted to reproduce electronic absorption and NRR spectra satisfactorily reproduce RR spectra too. In Figure 5 we report the RR spectra calculated in the three solvents for different excitation lines within the absorption band. In good agreement with experimental data,<sup>3,8</sup> the relevant band softens and broadens with increasing solvent polarity. Moreover the RR spectrum in apolar solvent, as modeled by  $\epsilon_{or} \sim 0.2$ , turns out to be fairly independent of the excitation line (panel A), while in polar solvents (large  $\epsilon_{or}$ , panels B and C) it shows a large dispersion with the excitation line.

## Discussion

The simple model for solvated push–pull chromophores presented in I gives a fairly good description of the solvent dependence of electronic absorption spectra, accurately reproducing the evolution with the solvent polarity of the frequency, intensity and band-shape (see Figure 2). It also explains the broadening and softening of NRR and RR bands with increasing solvent polarity (Figures 3 and 4), and reproduces the peculiar dispersion with the excitation line of the RR spectra in polar solvents (Figure 5, panels B and C). In view of the simplicity of the model and of the reduced set of adjustable parameters used, an impressive agreement between experimental and theoretical data is obtained, thus demonstrating that the model retains the essential physics underlying the spectral behavior of PB.

The large solvation effects observed in vibrational spectra of PB, and particularly the anomalous dispersion of RR bands with the excitation line, were previously ascribed<sup>9</sup> to the inhomogeneous broadening of both electronic and vibrational states. The correlation of electronic and vibrational energies, needed to reproduce the observed dispersion of RR frequencies



with the excitation line, was similarly recognized.<sup>8,9</sup> However the authors of refs 8 and 9, adopting a standard picture for the solute–solvent interaction, did not fully exploit the large nonlinearity of the PB molecule. As discussed in I, standard perturbative approaches to solvation only account for solvent-dependent molecular energies, but do not allow for corrections to the molecular wave functions. Then, in this rigid-solute picture, all molecular properties are solvent independent, so that, to account for inhomogeneous broadening of vibrational bands in polar solvents, the authors of ref 9 were forced to introduce an ad hoc interaction between internal vibrational coordinates and the effective solvation coordinate. This phenomenological approach has the merit of emphasizing the coupling between the two degrees of freedom, but it introduces one more arbitrary parameter that cannot be directly related to the physical properties of neither the solute nor the solvent molecule.

Our nonperturbative picture, by contrast, fully accounts for the large polarizability of the solute. We do not introduce any direct interaction between vibrational modes and solvation coordinates: the two motions are indeed correlated via their common interaction with electronic degrees of freedom. In a nonperturbative approach, the solvent affects chromophore energies and wave functions, so that it also affects vibrational properties. We have not introduced any ad hoc interaction, so that we are able to understand solvation effects in vibrational spectra in terms of the same basic interactions that govern electronic spectra, yielding a simple and internally consistent picture for all spectroscopical data. As a matter of fact our model also accounts for infrared (IR) spectra.<sup>6</sup> With the parameters in Table 2 we calculate the following IR absorption maxima: 1507, 1475, and 1462  $\text{cm}^{-1}$  in  $\text{CCl}_4$ ,  $\text{CHCl}_3$ , and DMSO, respectively. These frequencies are consistent with available experimental data<sup>8</sup> (the absorption frequency of PB in DMSO is covered by a strong solvent absorption). However we do not present a more extensive comparison of spectral band-shapes since, as proved by the spectroscopic analysis of isotopically substituted PB,<sup>8</sup> IR spectra are complicated, with respect to Raman spectra, by the appearance of an additional band, partly overlapping the  $\sim 1500 \text{ cm}^{-1}$  band.

In addition to electronic and vibrational properties, our model also accounts for NLO responses. The parameters in Table 2 in fact fix the relative magnitude of the static  $\langle \hat{\mu} \rangle \beta$  values as 1, 3.4, 4.3 in  $\text{CCl}_4$ ,  $\text{CHCl}_3$ , DMSO, respectively. This behavior is in good agreement with available experimental estimates<sup>5</sup> that locate the ratio of the static  $\langle \hat{\mu} \rangle \beta$  value in  $\text{CHCl}_3$  vs an apolar solvent (cyclohexane) as  $\sim 6$ . Once more the coupling to slow degrees of freedom (vibrations and solvation modes) plays an important role: in fact the purely electronic static  $\langle \hat{\mu} \rangle \beta$  values are unaffected within  $\sim 30\%$  by the solvent polarity, in striking disagreement with experimental data.

The mode appearing at  $\sim 1640 \text{ cm}^{-1}$  in the NRR spectra in Figures 3 and 4A, shows minor solvatochromic effects, with an overall softening, in the three solvents, of  $\sim 10 \text{ cm}^{-1}$ , to be compared with the much larger shift ( $\sim 30 \text{ cm}^{-1}$ ) observed for the  $\sim 1500 \text{ cm}^{-1}$  mode. Similarly, a small dispersion with the excitation line has been reported for this mode in RR spectra.<sup>8</sup> In the previous section, we focused attention on the largest spectral effects, and deliberately avoided discussing these small effects, just to keep discussion simple, and the number of microscopic parameters at a minimum. We can of course extend our model to account for the coupling of two vibrational modes. As detailed in I, in the multimode case, the frequency and intensity of each coupled vibration depend in a complex way from the frequencies and the coupling strengths of all vibrational

modes. Then, to reproduce experimental data including the effects observed for the  $\sim 1640 \text{ cm}^{-1}$  mode, not only an additional Holstein vibration has to be introduced, but also the parameters relevant to the other vibration have to be modified. Spectral data are well reproduced<sup>17</sup> by imposing  $z_0 = 0.8$ ,  $\omega_1 = 0.19$ ,  $\epsilon_1 = 0.12$ ,  $\omega_2 = 0.21$ ,  $\epsilon_2 = 0.39$ , i.e., by adopting the same parameters as in the upper panel of Figure 2 in I. It turns out that the lowest mode, that shows larger effects from solvation, is characterized by a much smaller relaxation energy than the higher mode: this is a fairly common situation, since in the multimode case, lower modes are the most strongly affected by electron–phonon perturbation, and borrow intensity from higher modes.<sup>2</sup> In this respect, modeling the spectral behavior of push–pull chromophores seems difficult because many modes can be coupled, but locating them can be very difficult since some of them, with possibly large couplings, can show up with fairly weak spectral signatures. Whereas this problem has to be kept in mind each time a detailed description of electron–phonon coupling is extracted from vibrational spectra, notably from RR spectra, we believe it does not hinder a reliable estimate of the most important parameters characterizing the chromophore. Indeed, the small polaron binding energy, i.e., the sum of the relaxation energies of Holstein vibrations, is approximately constant, independent of its partitioning in one or more coupled modes. Whereas the details of vibrational spectra can be modeled with increasing degree of accuracy introducing an increasing number of coupled modes, the essential physics remains unchanged.

When dissolved in protic solvent like  $\text{CHCl}_3$ , PB can easily participate in H-bonds, involving the O atom and the iminic and/or aminic N atoms. Then the observed softening and broadening of the bands at  $\sim 1500 \text{ cm}^{-1}$  (nominally the C=N stretch) and at  $\sim 1640 \text{ cm}^{-1}$  (nominally the C=O stretch) from  $\text{CCl}_4$  to  $\text{CHCl}_3$  can be, at least partly, assigned to H-bond formation. We believe, however, that H-bond plays only a minor role on vibrational spectra of PB in  $\text{CHCl}_3$ . In fact, the behavior in  $\text{CHCl}_3$  is fairly well consistent with the behavior observed in DMSO, a polar aprotic solvent, where, due to the higher polarity, actually larger effects are observed than in  $\text{CHCl}_3$ . Moreover, as suggested by the chemical intuition and further confirmed by ab initio calculations,<sup>19</sup> H-bond should be much more effective on the oxygen site. Indeed by far the largest spectral effects are observed for the C=N stretching vibration, ruling out H-bond as the main source of solvent effects in vibrational spectra of PB.

As a final comment, we underline that the present model applies with no major modifications to supercritical fluid solvents, with broadening of electronic and vibrational states affecting chromophores dissolved in polar solvents. In fact the dispersion of RR lines is only observed for PB dissolved in polar fluids. However, a more precise modeling of spectral properties of PB dissolved in supercritical fluids has to account for the role of the fast (electronic) degrees of freedom of the solvent.<sup>6</sup> When comparing the spectral properties of chromophores dispersed in solvents with very different physical properties, the dependence of the “solute” microscopic parameters (namely  $z_0$ ) on the solvent refractive index and density<sup>13</sup> cannot be disregarded.

## Conclusion

We have presented a systematic analysis of electronic absorption and vibrational spectra of PB dissolved in solvents with different polarity. All data fit quite naturally into the interpretative scheme presented in I, confirming its reliability.

The relevant physics is described in terms of two electronic states coupled with low-energy degrees of freedom, including molecular vibrations and the orientational degrees of freedom of polar solvents. Because of the intrinsic nonlinearity of the system, a correlation between slow modes arises from their common interaction with the electronic degrees of freedom. The consequences of this interaction mediated by the electronic states is of course small (and eventually negligible) in systems with very low or very high polarity. In these two extreme limits in fact the chromophore has an essentially linear behavior: perturbations linearly affect electronic energies and hardly propagate to other degrees of freedom. More interesting systems, like PB, have intermediate polarity: for such molecules the intrinsic nonlinearity of the two-state electronic model guarantees a good propagation of perturbations and an amplification of the coupling effects. Extending the analysis to other chromophores is certainly important to further test the reliability of the model and to define its applicability range. Even more, we believe that a systematic spectroscopic analysis of push-pull chromophores is an important step to get a real understanding of the behavior of materials for nonlinear optics.

**Acknowledgment.** We thank G. Dellepiane and A. Girlando for continuous encouragement and support of our work and for several useful discussions. Work supported by the Italian National Research Council (CNR) within its "Progetto Finalizzato Materiali Speciali per Tecnologie Avanzate II", and by the Ministry of University and of Scientific and Technological Research (MURST).

## References and Notes

- (1) Brooker, L. G. S.; Sprague, R. H. *J. Am. Chem. Soc.* **1941**, *63*, 3214.
- (2) Figueras, J. *J. Am. Chem. Soc.* **1971**, *93*, 3255.
- (3) Yamaguchi, T.; Kimura, Y.; Hirota, N. *J. Phys. Chem. A* **1997**, *101*, 9050.
- (4) Morley, J. O.; Fitton, A. L. *J. Phys. Chem. A* **1999**, *103*, 11442.
- (5) Marder, S. R.; Beratan, D. N.; Cheng, L.-T. *Science* **1991**, *252*, 103.
- (6) Painelli, A.; Terenziani, F. *J. Phys. Chem. A* **2000**, *104*, 11041 (jp0016075, previous paper in this issue).
- (7) Painelli, A.; Terenziani, F. *Chem. Phys. Lett.* **1999**, *312*, 211.
- (8) Yamaguchi, T.; Kimura, Y.; Hirota, N. *J. Chem. Phys.* **1998**, *109*, 9075.
- (9) Yamaguchi, T.; Kimura, Y.; Hirota, N. *J. Chem. Phys.* **1998**, *109*, 9084.
- (10) Painelli, A.; Girlando, A. *J. Chem. Phys.* **1986**, *84*, 5665.
- (11) Girlando, A.; Painelli, A.; Soos, Z. G. *Acta Phys. Pol. A* **1995**, *87*, 735.
- (12) Soos, Z. G.; Mukhopadhyay, D.; Painelli, A.; Girlando, A. *Handbook of Conducting Polymers*; Marcel Dekker: New York, 1998; p 165.
- (13) Painelli, A. *Chem. Phys.* **1999**, *245*, 183. Painelli, A. *Chem. Phys.* **2000**, *253*, 393.
- (14) Lu, D.; Chen, G.; Perry, J. W.; Goddard, W. A. *J. Am. Chem. Soc.* **1994**, *101*, 5860.
- (15) Kim, H.-S.; Cho, M.; Jeon, S.-J. *J. Chem. Phys.* **1997**, *107*, 1936.
- (16) Painelli, A. *Chem. Phys. Lett.* **1998**, *285*, 352.
- (17) Painelli, A.; Terenziani, F. *Synth. Met.*, in press.
- (18) Reynolds, L.; Gardecki, J. A.; Frankland, S. J. V.; Horng, M. L.; Maroncelli, M. *J. Phys. Chem.* **1996**, *100*, 10337.
- (19) Serrano, A.; Canuto, S. *Int. J. Quant. Chem.* **1998**, *70*, 745.